RESEARCH ARTICLE

Impact Assessment Framework for Grid Integration of Energy Storage Systems and Renewable Energy Sources Toward Clean Energy Transition

FARHAD ANGIZEH[1], **(Member, IEEE), JINWOO BAE**[1], **(Student Member, IEEE), JOYCE CHEN**[2], **ALEXANDER KLEBNIKOV**[2], **AND MOHSEN A. JAFARI**[1], **(Member, IEEE)**
[1]Department of Industrial and Systems Engineering, Rutgers, The State University of New Jersey, Piscataway, NJ 08854, USA
[2]Atlantic Shores Offshore Wind LLC, Brooklyn, NY 11205, USA

Corresponding author: Farhad Angizeh (farhad.angizeh@rutgers.edu)

ABSTRACT This paper proposes a two-stage decision-making tool to assess the impacts of energy storage systems (ESSs) and offshore wind farms (OSW) integration in the power grid. To quantify the potential impacts, various key performance indicators (KPIs) are incorporated. These KPIs gage the environmental, technical, and economical attributes of the integrated system. The proposed framework uses a unit commitment (UC) mixed-integer linear programming (MILP) model. Two case studies (one for New Jersey and one for New York) are examined with clean power transition targets. The uncertainties of the net-load and power generation from renewable energy sources (RESs) are characterized by Gaussian Process Regression (GPR) models. These models are fine-tuned using the base forecasts generated using our in-house load forecasting tool and the National Renewable Energy Laboratory's (NREL) publicly available generation calculator. The results show that ESS installations almost always improve the performance of the grid, regardless of the location and configuration. Furthermore, the unequally distributed ESS installations show better impacts than standalone centralized ESSs; and the mixed ESS technologies outperform single-type ESS deployments.

INDEX TERMS Clean energy transition, net-zero energy system, 100% renewable energy, sustainability, offshore wind (OSW), energy storage system (ESS), planning and operation optimization.

I. INTRODUCTION

Increasing the deployment of renewable energy sources (RESs) integrated with energy storage systems (ESSs) has become one of the widely accepted practices to decarbonize the supply-side of power grid by gradually substituting conventional generating units [1]. The transition from current fossil-fueled-dominated systems to 100% clean power grids is quite a challenging task. This paper aims to answer the question of "How to strategically implement techno-economically viable and environmentally friendly scenarios aligned with the planned interim phases?" To address this problem, a set of tools to assess the merits of the potential strategies are essential. These tools must be capable of incorporating the unique geographical and network-related features and targeted plans which vary from one region to another region in the country.

There have been some research works in the literature addressing the challenges and opportunities of the clean energy transition planning problem. The National Renewable Energy Laboratory's (NREL) study in [2] uses its publicly available Regional Energy Deployment System capacity expansion model to investigate supply-side scenarios to a

The associate editor coordinating the review of this manuscript and approving it for publication was Chenghong Gu.

net-zero power grid by 2035, considering least-cost options. In [3], the authors propose a two-factor learning curve model to analyze the impact of innovation and deployment policies on the cost of energy storage technologies over time from an empirical dataset. Reference [4] reviews Southeast Asia's energy sector trends, focusing on electricity supply and demand, highlighting the crucial role governments and public policy can play in accelerating the region's clean energy transition. Khan et al. generate and measure a principal components index in [5] as an independent variable to capture the effects of the clean energy transition on crucial trade-offs between economic growth and environmental sustainability. An integrated method to explore the environmental impacts of robust energy policy mixes towards clean energy transitions is proposed in [6]. The literature, however, lacks sufficient evaluation tools to guide policymakers and developers to evaluate and validate various potential scenarios for maximum value generation.

In that context, this paper proposes a novel integrated impact-assessment framework to quantify the potential impacts of ESSs and RESs integration scenarios. The proposed framework, which is developed on a Unit Commitment (UC)-based optimization model, encompasses a heuristic two-stage process to assess various impacts of ESSs and RESs integration using a set of key performance indicators (KPIs). The employed KPIs measure grid characteristics, including technical/engineering, economical, and environmental aspects. The built-in UC-based model co-optimizes the day-ahead hourly schedules of conventional/renewable generating units and candidate ESSs with their corresponding dispatch/injection and charging/discharging levels to balance supply and projected demand without contravening the transmission network constraints. ESS sizing and siting are also decided. To characterize the uncertainty of the RESs and projected demand, a set of fine-tuned Gaussian Process Regression (GPR) models are utilized. The value metrics can be measured from both the grid operator's and individual developer's perspectives, though this paper only taps into the grid values and leaves the latter for future work. Two case studies are demonstrated to reveal the practicality of the proposed impact-assessment framework. One case study is for the state of New Jersey (NJ), where the Energy Master Plan (EMP) of 2019 calls for a 100% clean power grid by 2050. The second case study is for the state of New York (NY) with its Climate Act of 2019 that involves ESSs and OSWs integration targets and sets the state to pursue a net-zero clean power grid by 2040.

In summary, the core contributions of this paper include:
- A set of KPIs, including economic, environmental, and technical/engineering value factors, to quantify the potential impacts of integrating ESSs and RESs in the power grid. These KPIs are intended to provide insights for decision-makers to strategically implement the validated scenarios,
- An hourly operation scheduling tool on a UC-based optimization model that incorporates the planned gener-

ation fleet expansion/deactivation and RESs generation and net-load forecasts to carry out reliable day-ahead supply-demand balance plans, and
- A benchmark test and evaluation system for both New Jersey and New York States using publicly available databases. The developed benchmarks unlock further investigations, such as energy policy and regulations, market mechanisms, and pricing/incentive programs.

The remainder of this paper is organized as follows: The proposed UC-based impact-assessment framework and uncertainty characterization of RESs are elucidated in Section II. The mathematical formulation is detailed in the Appendix. Section III represents the numerical experiments for the New Jersey and New York case studies. Finally, the conclusions are drawn and discussed in Section IV.

II. UC-BASED IMPACT-ASSESSMENT FRAMEWORK
Here a two-stage UC-based approach is employed to assess the impacts of different integration scenarios using a set of KPIs. But prior to delving into the specifics of the proposed two-stage approach, let us first lay the groundwork by discussing the generic UC model and further clarify the KPIs selection and measurement.

A. PROBLEM FORMULATION AND KPI SELECTION
The generic form of the UC model that aims to minimize the total operation cost of a system is formulated as:

$$\min_{\mathbf{G},\mathbf{I}} \quad F(\mathbf{G},\mathbf{I}) \tag{1}$$

$$\text{s.t.} \quad \mathbf{f}(\mathbf{G},\mathbf{I}) = 0 \quad (\mathbf{\Lambda}) \tag{2}$$

$$\mathbf{h}(\mathbf{G},\mathbf{I}) \leq 0 \quad (\mathbf{\Pi}) \tag{3}$$

$$\mathbf{G} \in \mathbf{\Omega} \tag{4}$$

where $F(\cdot)$ is the total operation cost with $\mathbf{G}$ and $\mathbf{I}$ to be generating units' dispatch and commitment variables, respectively. $\mathbf{f}(\cdot)$ and $\mathbf{h}(\cdot)$ are equality, e.g., power balance equations, and inequality, e.g., generation limits, constraints with respectively corresponding Lagrange multiplier matrices $\mathbf{\Lambda}$ and $\mathbf{\Pi}$. Also, $\mathbf{\Omega}$ denotes the feasible region of the generating units. In our proposed framework, the generic model presented in (1)-(4) is reconstructed by incorporating RESs availability and ESSs operation models, transmission network constraints, and the system's reserve requirements, which are detailed in the Appendix. The built-in UC-based model co-optimizes the most economical set of power generating units, dispatches the available RESs, i.e., wind and solar farms, and schedules the charging/discharging of the ESSs to meet the day-ahead demand forecast. It also sets aside sufficient capacities to supply the required system reserves.

As discussed in Section I, a set of KPIs that measure grid characteristics is essential to quantify the potential impacts of RESs and ESSs integration scenarios. With this in mind, five KPIs are selected and measured, including (i) Total operation cost, (ii) Locational marginal prices (LMPs), (iii) Transmission lines congestion/loading, (iv) Renewable

energy curtailment, and (v) Carbon footprint. Total operation cost and LMP directly measure the economical aspect of the grid where the former is the optimal value of the objective function (see (5) in the Appendix) and the latter is the Lagrange multiplier of the power balance equation—that is formulated in (23) in the Appendix. Transmission loading and renewable energy curtailment, which both measure the technical/engineering aspect of the grid, are directly calculated from the decision variables designated for the transmission line flows P_{lt} and the RESs' deployments, i.e., P_{wt} and P_{st}, in the Appendix. Lastly, the carbon footprint is selected to measure the environmental aspect of the grid, which is also calculated from the decision variable modeling the optimal dispatches of the conventional generating units, i.e., P_{gt} in the Appendix, using their corresponding emission rates adopted from the U.S. Energy Information Administration (EIA) database [15].

Now that the built-in UC-based model is elaborated and the KPIs selection and measurement are clarified, the proposed two-stage impact-assessment approach is detailed. In the first stage, an hourly UC-based optimization model is simulated. The simulation takes for input the target year's infrastructure data, including the techno-economic data of the projected generation fleet with planned expansions/deactivations, transmission network data, and forecasted demand, including the massive impact of planned offshore wind farms off the coast of New York and New Jersey, but not assuming any new ESS installations. This constructs the Baseline analysis to measure the five KPIs.

Next, the measured KPIs are analyzed, and based on the LMPs, congested transmission zones, and renewable curtailments, a set of candidate sweet spots are offered to install new ESSs. In the second stage, the model is rerun multiple times with different ESS deployment scenarios considering various configurations obtained from the feasible permutations of the candidate locations given the aggregate planned capacities. Finally, the KPIs are measured again to observe the impacts and compared with Baseline measurements to assess the validated scenarios. Fig. 1 illustrates the two-stage procedure to quantify the potential impacts of the ESSs and OSWs integration.

The ESSs deployment scenarios includes cases with a single centralized ESSs in each candidate location and cases with multiple distributed ESSs given the planned aggregate capacities. In the distributed ESSs, both equal and unequal capacities in different locations are analyzed. This allows a quantified comparison between different types of ESS technology. Furthermore, the impacts of mixes of different technologies are analyzed to investigate the effectiveness of diversifying the new ESS installations.

B. UNCERTAINTY CHARACTERIZATION

The projected demand and RESs generations are two main input parameters with inherent stochasticity. The nodal hourly demand profiles are forecasted over the planning target years using our in-house high-resolution demand forecasting tool [7]. The NREL's PVWatts Calculator [8] is utilized to generate a set of preliminary hourly profiles for on-land wind and solar photovoltaic (PV) powers in different locations across the two states. To estimate hourly OSW power productions over the target years, a 3-day raw data is extracted for each season from the publicly available wind speed database in [9]. To inject more variability, the forecasting horizon is expanded to span over a 7-day representative period; the 7-day data is randomly generated from the 3-day raw data by random sampling through Gaussian Process Regression (GPR) [10]. The GPR model captures the mean of the data in the same hours and the covariance of each hourly data in a day. Then, random sampling is conducted to generate the hourly 7-day data based on the functions with 95% prediction interval. To investigate the effectiveness of the proposed model, numerical experiments are conducted next.

TABLE 1. Technical characteristics of ESS technologies.

Technology	Parameters	
	Discharge Duration	Round-trip Efficiency
Li-ion Battery	4-hr	87.6%
	2-hr	87.6%
VF Battery	8-hr	74.0%
Hydrogen FC	10-hr	35.0%

III. CASE STUDY AND NUMERICAL EXPERIMENT

Two case studies are investigated to delineate the efficacy of the proposed impact assessment framework: Case I for New Jersey State and Case II for New York State. The New Jersey Energy Master Plan (EMP) [11] follows a path to 100% clean energy by 2050. The New Climate Leadership and Community Protection Act (CLCPA) [12] sets the New York State on a path to reaching net-zero greenhouse gas (GHG) emissions by 2040. For both cases, our analysis includes all the expected targeted changes in the network (e.g., expansion of renewable sources and retirement assets with GHG footprints). The projected changes in electricity load due to the increasing penetration of Electric Vehicles are also included. For ESS configuration, multiple scenarios are considered, including centralized and distributed, with equal and unequal distributed capacities. For distributed configurations, different sets of candidate ESS locations and capacities are explored. Regarding the ESS technologies, three types are considered: Li-ion battery, vanadium flow (VF) battery, and hydrogen fuel cell (FC). Additionally, various mixes of these technologies are analyzed. It should be noted that the three ESS technologies modeled were selected as most likely to be deployed varieties, after comprehensively evaluating sixteen total ESS technologies. The characteristics of the suggested top three ESS technologies are presented in Table 1.

The optimization models for the two case studies have slight differences in formulation and input data. Both models were implemented and solved using CPLEX 12 solver under
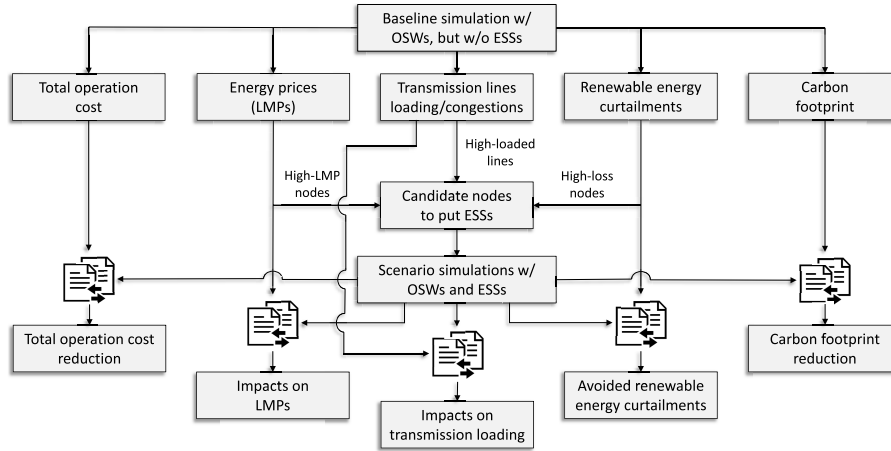
FIGURE 1. Proposed two-stage UC-based framework with the 5 KPIs.

TABLE 2. NJ's planned OSW Farm installation with rated capacity, POI, and expected COD.

OSW Project	Rated Capacity [MW]	POI	Expected COD
A	816	b8	2025
B	432	b11	2025
C	1,510	b7	2028
D	1,148	b10	2030
E	1,200	b10	2030
F	1,200	b11	2035
G	1,342	b14	2035

GAMS [13] on a desktop computer with a Core i7-11800H processor at 2.30 GHz and 16 GB of RAM.

A. CASE STUDY I: NEW JERSEY POWER TRANSMISSION GRID

1) TEST SYSTEM AND INPUT DATA

New Jersey is committed to building 7,500 MW of OSW, 17,000 MW of solar energy, and 2,500 MW of ESS by 2035, with ambitious interim targets of 3,500 MW of OSW and 2,000 MW of ESS by 2030. Moreover, the State's EMP plans to fulfill a set of demand-side electrification activities, including 330K EVs on the road by 2025 and 2M by 2035 and 400 MW per year of behind-the-meter solar PV through 2030. The above-mentioned demand-side parameters are fed into the net-load forecasting tool to estimate the hourly nodal demand profiles over the planning years, which is elaborated in [7].

The NJ's power grid is part of the PJM interconnection, and to assure sufficient accuracy in the analyses, a county-level representative transmission network is selected to mimic the state's power grid. Fig. 2 illustrates NJ's representative 30-bus power transmission grid with the planned OSW interconnections. The state's planned OSW farms with their corresponding rated capacities, point-of-interconnections (POIs), and expected commercial operation date (COD) are implemented as presented in Table 2.

As can be seen from Fig. 2, nine interconnections are considered between NJ and the neighboring states, i.e., Pennsylvania (b22–b24), Delaware (b25), and New York
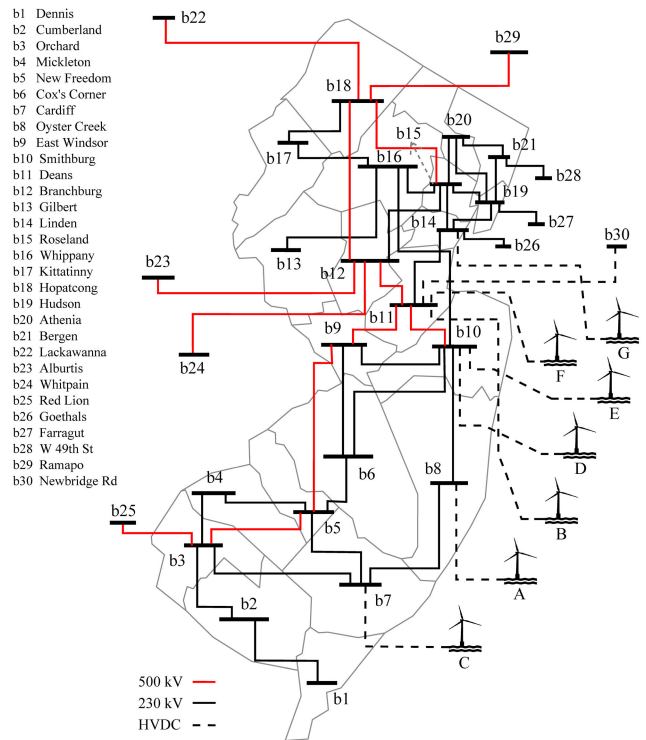

FIGURE 2. NJ's 30-bus representative transmission network with its planned OSWs at A–G expected to be operational between 2025 to 2035.

(b26–b30) states that are notably important to balance supply and demand. Finally, the generation fleet data, including techno-economic data for each power plant and the state's expansion/deactivation plans, are adopted from PJM [14] and the U.S. Energy Information Administration (EIA) [15] databases. The in-state county-level aggregate generation capacities, primarily natural gas and nuclear power, are shown in Fig. 3 for the year 2018.

The analyses are carried out over four target planning years, 2025, 2028, 2030, and 2035. In each planning year, the state's target aggregate capacity is used with
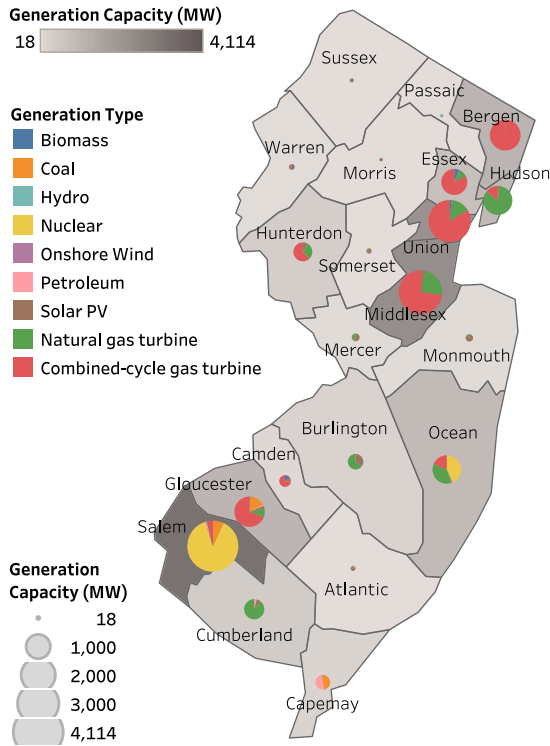
FIGURE 3. New Jersey's county-level aggregated generation mix and capacities in MW in 2018.

TABLE 3. Selection criteria and candidate buses for ESS siting.

Candidate Bus	Selection Criteria		
	High-LMP Bus	High-Loaded Transmission Line	Renewable Curtailment
b19	✓	✓	
b20	✓		
b21	✓		
b15		✓	
b17		✓	
b18		✓	
b7			✓
b10			✓

yearly capacity increments following the NJ targeted ESS installation plans including: 600 MW in 2025; 1,200 MW in 2028; 2,000 MW in 2030; and 2,500 MW in 2035. For each scenario, an incremental analysis that shows the impact of the partial capacity of the State's target are carried out. This provides insight into the additional value of the individual ESS investments done by private developers. The net-load and RES power generation forecasts are made over a 7-day period for four seasons. For each season, a representative month is selected: January (Winter), April (Spring), July (Summer), and October (Fall). The forecasts are made using our in-house developed load forecasting tool and the GPR (see Section II-B). The KPIs are measured for each period and averaged to find the weekly average values over a planning year.

2) RESULTS AND DISCUSSIONS
As discussed in Section II, the ESS siting selection criteria, including (i) high LMPs, (ii) high-loaded transmission lines,

TABLE 4. KPIs of the baseline scenarios.

KPI	Planning Year			
	2025	2028	2030	2035
Highest-spike LMP [$/MWh]	70.48	92.81	47.41	63.39
Avg. LMP in Peak Times [$/MWh]	47.51	44.84	36.09	30.01
Avg. Transmission Loading on Congested Lines in Peak Times [%]	64.26	63.53	67.61	65.02
Total Operation Cost [million dollars]	36.32	29.84	24.83	20.28
Renewable Curtailment [MWh]	0	10,398	43,615	356,803
Carbon Footprint [Short Ton]	540,846	434,076	344,024	258,050

and (iii) renewable curtailments, or high-loss buses, yields eight candidate buses that are presented in Table 3. Note that the candidate buses are consistent with the findings reported in our previous work in [16], where a UC-based optimization model was reconstructed with additional decision variables to find the optimal siting for an aggregate 600 MW of ESSs with 4-hr discharge duration.

Table 4 provides the average KPIs of the baseline scenarios in each planning year.

The LMP and the transmission loading are divided into daily peak and off-peak times to demonstrate the impact of the ESS more effectively. The ESS is a sink node drawing power during off-peak times, demanding more generating units and transmission lines capacity utilization. However, the ESS turns out to be a source node releasing its stored energy during peak times and partially/ fully substitutes high-cost generating units and alleviates transmission congestion. Thus, assessing the integration impacts in peak and off-peak times provides more accurate results.

Next, the second-stage simulations are rendered to assess the impacts of planned ESS installation scenarios with different locations, configurations, and capacities. Table 5 shows the 7-day average impact-assessment results for twenty-one ESS scenarios in July 2028.

The simulation results show that the ESS installation improved the KPIs by reducing the curtailment of low-cost renewable energy generation. In most scenarios, distributed ESS configurations lead to relatively better KPIs than centralized ESSs. Furthermore, unequal capacity installations have better KPIs than the equally-distributed ESSs. Except for the transmission congestion KPI that reflects the transmission network capacity utilization, all the other KPIs are improved with ESS, regardless of location. It is observed that ESS relieves transmission load in some highly congested areas/zones and indirectly increases congestion in others. Since our results are inconclusive and do not show a generalizable improvement trends regarding transmission loading and congestion, our analysis will be focused on the remaining four KPIs.

To investigate the impacts of different ESS technology, multiple mixed technology scenarios are examined. Fig. 4 shows the measured KPIs for each technology mix, where the ratio refers to the rated capacities of Li-ion (with 4-hr discharge duration), vanadium flow, and hydrogen out of the total aggregate ESS capacity.

TABLE 5. The Measured 7-day average KPIs for 21 ESS scenarios in July 2028.

KPI \ Scenario		Baseline	1.1	1.2	1.3	1.4	1.5	1.6	1.7	1.8	2.1	2.2
ESS Allocation [Bus #(Cap. in MW)]		No ESS	b15(1,200) —	b17(1,200) —	b18(1,200) —	b19(1,200) —	b20(1,200) —	b21(1,200) —	b7(1,200) —	b10(1,200) —	b15(600) b18(600)	b15(600) b20(600)
Highest-spike LMP [$/MWh]		92.50	92.50	92.49	98.29	75.00	76.06	75.00	109.04	85.43	125.24	64.47
Avg. LMP [$/MWh]	Peak	49.64	54.59	46.22	43.61	45.69	45.03	45.75	41.55	42.86	45.85	44.27
	Off-Peak	28.15	27.91	28.01	27.90	28.42	28.12	28.27	28.07	27.83	27.84	27.82
Avg. Transmission Loading On Congested Lines [%]	Peak	67.99	67.05	67.07	68.14	66.82	67.97	67.60	74.27	69.99	67.65	68.15
	Off-Peak	66.01	66.79	67.19	66.19	64.39	65.03	65.13	64.28	65.43	66.82	66.93
Total Operation Cost [million dollars]		46.89	45.65	45.67	45.66	45.73	45.65	45.69	45.69	45.71	45.65	45.58
Renewable Curtailment [MWh]		3,520	3,507	3,544	3,494	3,563	3,528	3,625	9	3,498	3,500	3,489
Carbon Footprint [Short Ton]		733,458	735,238	735,485	735,349	734,330	734,866	734,760	733,833	735,190	735,301	735,241

KPI \ Scenario		2.3	2.4	2.5	3.1	3.2	3.3	3.4	3.5	3.6	4.1	4.2
ESS Allocation [Bus #(Cap. in MW)]		b20(600) b21(600) —	b15(800) b20(400) —	b15(400) b20(800) —	b15(400) b18(400) b20(400)	b15(400) b20(400) b21(400)	b15(600) b18(400) b20(200)	b15(200) b18(400) b20(600)	b15(600) b20(200) b21(400)	b15(200) b20(600) b21(400)	b7(120) b15(360) b18(360) b20(360)	b7(120) b15(360) b20(360) b21(360)
Highest-spike LMP [$/MWh]		74.97	62.44	86.14	86.14	61.43	90.81	86.14	60.56	60.56	73.76	75.72
Avg. LMP [$/MWh]	Peak	46.10	43.32	46.99	46.99	43.07	45.68	46.99	42.83	42.83	45.82	45.28
	Off-Peak	27.88	27.84	27.78	27.78	27.78	27.79	27.78	27.78	27.78	27.82	27.86
Avg. Transmission Loading On Congested Lines [%]	Peak	68.04	68.05	68.27	68.45	67.68	67.84	68.46	66.81	69.23	68.97	70.16
	Off-Peak	65.29	65.29	66.47	66.31	65.00	66.40	66.03	66.71	66.27	66.53	65.99
Total Operation Cost [million dollars]		45.63	45.63	45.63	45.63	45.63	45.64	45.63	45.63	45.63	45.59	45.63
Renewable Curtailment [MWh]		3,492	3,490	3,560	3,556	3,489	3,529	3,556	3,489	3,489	2,148	2,173
Carbon Footprint [Short Ton]		735,075	735,175	735,050	735,064	735,339	735,232	735,082	735,371	735,362	734,450	734,378

FIGURE 4. Measured KPIs for different ESS technology scenarios including mixed technologies.

other hand, the flow battery technology is most effective in LMP reduction. A technology mix of the two can alleviate the shortcomings of the individual technologies. Based on our results, the technology mixes of (8:1:1) and (7:1.5:1.5) provide more reduction in the renewable energy curtailment than single-type technologies and still show almost the same effectiveness compared to the best single-type technology scenarios in the other KPIs.

Putting together all the simulation results obtained from the four target planning years, Fig. 5 demonstrates the potential strategic ESS implementation roadmap from 2025 to 2035, given the target ESS aggregate capacities. As can be seen from this figure, different pathways can be selected depending on the most important KPI selected by the decision makers. The red, blue, green, and yellow arrows represent the "optimal" pathways based on the total operation cost, carbon footprint, renewable energy curtailment, and average LMP during peak times, respectively.

B. CASE STUDY II: NEW YORK POWER TRANSMISSION GRID

1) TEST SYSTEM AND INPUT DATA

The state has set targets including 6,000 MW of solar by 2025, 70% RESs by 2030, 9,000 MW of OSW by 2035, 85% reduction in GHG emissions from 1990 levels by 2050, and 3,000 MW of ESSs by 2030. The NY's eleven control area load zones are considered to model the state's representative power transmission grid. Fig. 6 depicts the NY's representative 27-bus power transmission grid with the state's planned OSW interconnections. Table 6 provides the state's planned OSW farm characteristics. In Fig. 6, sixteen interconnections are considered between the NY and its neighboring utilities/markets, including PJM (b12–b19), the Independent Electricity System Operator (IESO) which is Ontario's power system (b20), Hydro-Quebec (b21–b23), and New England Independent System Operator (ISONE) with (b24–b27). The generation fleet data and the state's
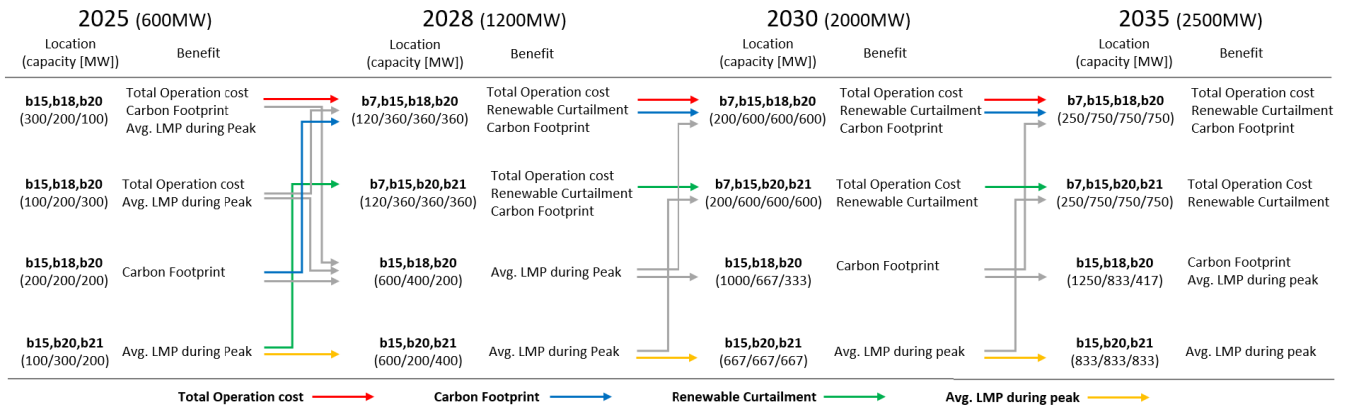
From the analysis, a 4-hr Li-ion battery shows the highest reduction in the total operation cost by 5% and the carbon footprint by 4%, while a vanadium flow battery is the most effective technology that decreases the average LMP during the peak time (by 19%). The hydrogen FC shows the slightest reduction in all the KPIs due to its low round-trip efficiency that leads to energy losses despite its large energy capacity.

The mixed technology scenarios provide higher effectiveness in reducing the curtailment of renewable power generation. For the other KPIs, single and mixed technologies perform similarly. For instance, Li-ion battery provides the best performance in total operation cost and carbon footprint, and low performance in reducing LMP. On the

FIGURE 5. Strategic ESS implementation roadmap from 2025 to 2035 given the target ESS aggregate capacities.
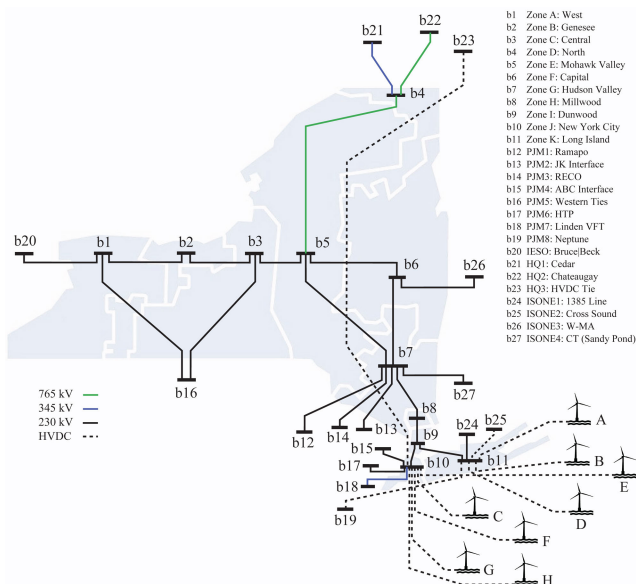

FIGURE 6. NY's 27-bus representative transmission network with its planned OSWs at A–H expected to be operational from 2023 to 2035.

TABLE 6. NY's Planned OSW Farm Installations With Rated Capacity, POI, and Expected COD.

OSW Project	Rated Capacity [MW]	POI	Expected COD
A	130	b11	2023
B	880	b11	2025
C	816	b10	2026
D	1,260	b11	2027
E	1,230	b10	2028
F	1,200	b10	2031
G	2,000	b10	2033
H	1,700	b10	2035

generation expansion/deactivation plans are adopted from the New York Independent System Operator's (NYISO) *2022 Gold Book* [17]. The hourly nodal net-load and the RES generation forecasts for the target planning year are estimated using similar tools used for the NJ case study.

In contrast to the NJ study, the NY case is carried out for a single target year 2030; but with multiple planned aggregate ESS capacities to reflect possible optimistic and pessimistic scenarios alongside the state's actual planned capacity, which is 3,000 MW. Accordingly, four different aggregate ESS capacities of 500, 1,000, 3,000, and 6,000 MW are examined. Additionally, the ESS siting is assumed to be restricted to either zone J (b10) or K (b11) to comply with the New York State Energy Research and Development Authority's (NYSERDA) 2022 offshore wind solicitation requirements [18]. The Li-ion battery ESS with a 4-hr discharge duration and 87.6% round-trip efficiency is considered for the primary analysis. The simulation time horizon is the same 7-day representative in two Winter and Summer seasons, where the net-load and RES generation forecasts are obtained following the same methods explained for the NJ study.

In order to investigate the potential impacts on the grid from a single developer's perspective, an additional set of relatively small ESS capacities, e.g., 20 and 40 MW, are also considered. These capacities are on top of the State's targeted plans. These incremental ESS installations, from a developer's perspective, provide valuable insights to developers on the marginal impacts their projects would have on the grid.

2) RESULTS AND DISCUSSIONS

Table 7 shows the 7-day average measured KPIs in the baseline scenarios for the four target aggregate ESS capacities in 2030. Note that the location configuration consists of pre-installed capacities only in Zone J, only in Zone K, and equally-distributed in Zones J and K. Next, the ESS deployment scenarios are simulated and the KPIs are measured and compared to the baseline results. Fig. 7 shows the 7-day average impact-assessment results in 2030 for different Li-ion battery ESS scenarios of 4-hr discharge duration.

The simulation results reveal that over 90% of scenarios examined produce positive impacts due to ESS installation. Also, the KPIs compared to the baseline reduce the peak LMP by an amount between 0.5%–6% with the highest LMP by an amount between 10%– 60%, peak transmission congestion

TABLE 7. Average 7-day KPIs in different locations and target aggregate ESS capacities.

KPI	[No ESS] Baseline	ESS Allocation								
		500 MW			1,000 MW			3,000 MW		
		J	K	J,K*	J	K	J,K	J	K	J,K
Avg. LMP during peak [$/MWh]	46.27	-0.4%	+0.3%	-3.5%	+0.2%	+0.1%	-4.2%	-1.0%	-1.0%	-4.4%
Avg. transmission loading on congested lines during peak [%]	82.89	+4.0%	+2.9%	+4.7%	+3.5%	+2.1%	+3.9%	+6.2%	+1.7%	+4.5%
Total operation cost [million dollars]	71.83	-1.1%	-1.1%	-1.1%	-2.1%	-2.1%	-2.1%	-5.6%	-5.4%	-5.7%
Renewable curtailment [MWh]	29,768	-1.5%	-1.5%	-1.5%	-2.4%	-3.7%	-2.4%	-2.8%	-6.7%	-5.9%
Carbon footprint [Short Ton]	568,097	-1.1%	-2.3%	-0.9%	-1.3%	-1.4%	-1.2%	-2.4%	-2.5%	-2.8%

*Aggregate ESS capacities are equally distributed in "J,K" scenarios.

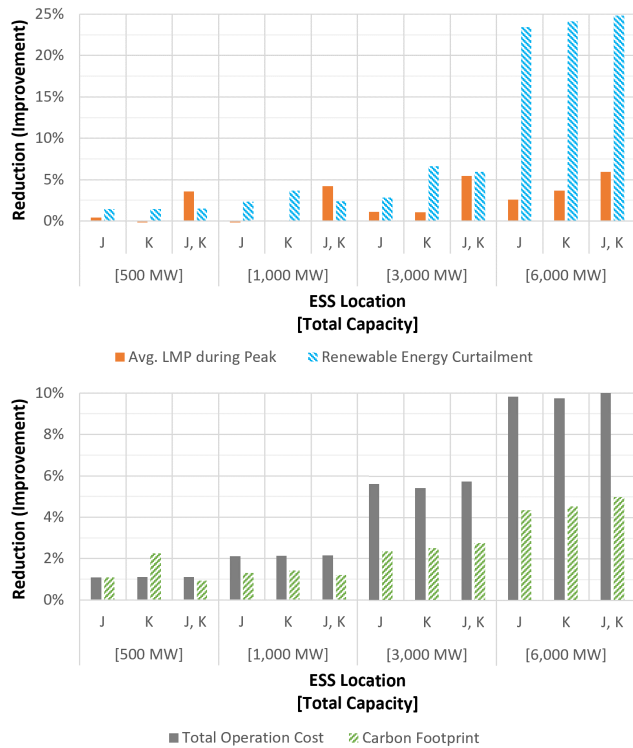**FIGURE 7.** Measured 7-day average KPIs for different aggregate ESS capacities located at Zones J or K or both in 2030.

FIGURE 8. Average Measured KPIs for different ESS scenarios including mixed technologies.

by an amount between 0.5%–1.5%, total operation cost by an amount between 1%–10%, renewable energy curtailments by an amount between 1.5%–25%, and carbon footprint by up to 5%. The ESS in Zone K represents more decrease in renewable energy curtailment, whereas the ESS in Zone J shows the tendency to decrease LMP during the peak times. Zone K also reduces the total operation cost more than Zone J when the capacity is 3,000 MW, although other capacities have no significant difference. The distributed ESSs have shown even more decreases in the LMP, total operation cost, and carbon footprint compared to the centralized standalone ESSs. It should be noted that the reported ESS capacities, e.g., 3,000 MW, are the aggregate capacities of multiple ESS projects located in the same zone if not configured as distributed ESSs. In other KPIs, the distribution of the ESS capacities provides an offset of the two zones. Furthermore, the incremental increases in ESS capacity positively impact these five measures. Regardless of
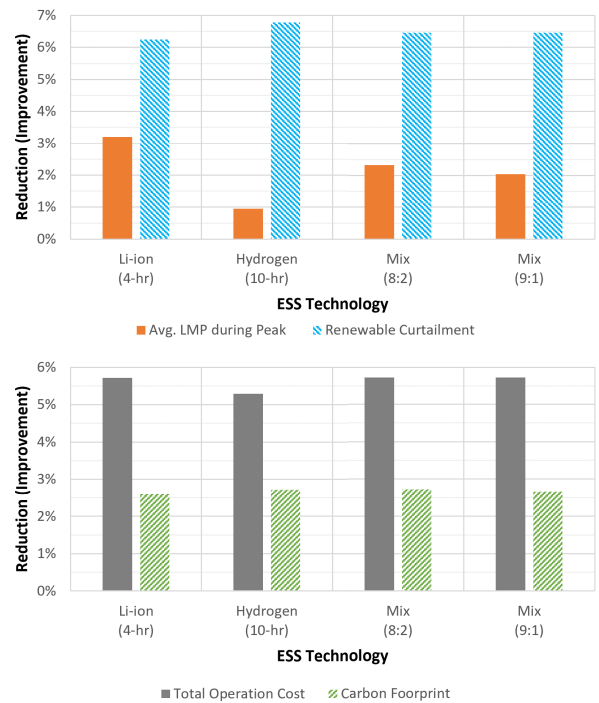
locations and configurations, it seems that ESS installations almost always improve the baseline KPIs. There are a few scenarios showing the ESS at either J or K zones may result in higher peak LMP and transmission congestion loading for higher ESS capacities. High congestion triggers the use of more expensive generators, thereby increasing the average peak LMP. Off-peak LMPs may also increase due to the demand generated by ESS charging at off-peak times.

Fig. 8 shows the impacts of ESS technologies, Li-ion battery, hydrogen storage, and their mix technology scenarios. As can be observed from Fig. 8, Li-ion battery with a 4-hr discharge duration seems to have better impacts than Hydrogen storage in economical-related KPIs; however, Hydrogen storage shows better results in carbon reduction and avoiding renewable curtailments. The results also prove that the technology mix can lead to better KPIs than single-type ESS deployments.

Table 8 provides the assessment results of incremental ESS impacts on the KPIs by adding a 20 MW or a 40 MW ESS on

TABLE 8. Observed average KPI improvements by additional incremental capacities to the already-installed aggregate 3,000 MW ESS.

Scenario \ KPI	Capacity [MW]	Avg. LMP [$/MWh]			Avg. transmission loading [%]		Renewable curtailment [MWh]		Total operation cost [million dollars]	Carbon footprint [Short Ton]
		Highest-spike	Peak	Off-Peak	Peak	Off-Peak	Solar & Wind	OSW		
J / K	3,000 / 0	70.00	45.79	34.98	88.07	79.72	28,926	0	67.78	554,605
+20 MW in J	3,020 / 0	+56.91%	-2.00%	+0.35%	+0.76%	-0.35%	-0.98%	0.00%	-0.02%	-0.01%
+20 MW in K	3,000 / 20	+16.23%	-3.29%	+0.31%	+0.55%	-0.51%	-0.95%	0.00%	-0.05%	-0.14%
+40 MW in J	3,040 / 0	+58.68%	-1.66%	+0.45%	+0.42%	-0.40%	-0.46%	0.00%	-0.07%	-0.17%
+40 MW in K	3,000 / 40	0.00%	-4.16%	+0.11%	+0.73%	-0.39%	-1.64%	0.00%	-0.08%	+0.04%
J / K	0 / 3,000	70.00	45.81	34.95	78.78	75.86	27,786	0	67.93	553,668
+20 MW in J	20 / 3,000	0.00%	-0.59%	+1.22%	+1.00%	-0.22%	+0.51%	0.00%	-0.04%	-0.03%
+20 MW in K	0 / 3,020	0.00%	-3.40%	-0.33%	+1.17%	+0.13%	+0.51%	0.00%	-0.02%	0.00%
+40 MW in J	40 / 3,000	0.00%	-3.71%	+0.54%	+1.54%	-0.15%	0.00%	0.00%	-0.10%	-0.12%
+40 MW in K	0 / 3,040	0.00%	-1.16%	+1.11%	+2.10%	+0.22%	+0.07%	0.00%	-0.06%	-0.07%
J / K	1,500 / 1,500	70.00	43.78	35.11	86.58	80.52	28,002	0	67.70	552,348
+20 MW in J	1,520 / 1,500	0.00%	-0.59%	-0.37%	+0.02%	+0.02%	-0.85%	0.00%	-0.04%	+0.06%
+20 MW in K	1,500 / 1,520	0.00%	-0.88%	-1.17%	+0.71%	-2.90%	+0.03%	0.00%	-0.03%	-0.02%
+40 MW in J	1,540 / 1,500	0.00%	-0.05%	-0.23%	-0.55%	-0.01%	-0.05%	0.00%	-0.06%	-0.05%
+40 MW in K	1,500 / 1,540	0.00%	-0.04%	+0.31%	+0.46%	-2.68%	-1.28%	0.00%	-0.08%	+0.07%

top of what is already installed, which is 3,000 MW in this case.

Overall, the capacity addition decreases the LMPs during peak times, renewable energy curtailment, total operation cost, and carbon footprint. As can be seen from the table, the renewable curtailment from OSWs is zero in the baseline scenarios. This comes from the fact that the generated power from the OSWs is fully utilized to supply the demand and charge the ESSs where the connecting transmission lines have sufficient headroom. Moreover, the results show that adding a small incremental ESS to a zone without an existing ESS further reduces the total operation cost due to the better impact of distributed ESSs on transmission congestion relief that avoids longer power transfers compared to the centralized ESSs. Adding 40 MW in Zone K seems more effective in reducing the LMPs during peak times. Under the distributed ESS scenarios, the location and capacity of the incremental ESS installations become more influential factors. Adding a 20 MW to Zone K is the most efficient scenario to relieve the LMPs during peak times, while adding a 40 MW to Zone J is more effective in decreasing carbon footprint. Also, adding a 40 MW to Zone K shows the most effective scenario to improve renewable curtailment and total operation cost.

IV. CONCLUSION

This paper proposed a two-stage UC-based impact-assessment framework that evaluates the impact of new OSW generation and different ESS technologies, using five KPIs. This framework could be usefully applied in future work to any energy markets, to evaluate the impacts of changing demand, new ESS additions, or major RES deployments, or any combination of those events. New Jersey and New York states, with their ambitious clean power grid targets, were investigated. The simulation results revealed that over 90% of the scenarios examined produce positive impacts due to ESS installations. Furthermore, Li-ion batteries with a 4-hr discharge duration showed better impacts in all KPIs than flow batteries with 8-hr and hydrogen storage with 10-hr, except for average peak LMPs where the flow battery provided better results. Additionally, diversifying ESS technologies can lead to better KPIs

than single-type ESS deployments. In terms of the ESS configuration, distributed capacities generated better KPIs than centralized standalone ESSs, and unequally distributed cases outperformed the equally-distributed configurations. Finally, it was observed that regardless of the locations and configurations, ESS installations almost always improve the baseline KPIs in both studies.

APPENDIX
UC-BASED MODEL

The objective function of the proposed UC-based model to be minimized is:

$$\sum_{t\in\mathcal{T}}\left[\sum_{g\in\mathcal{G}}\left(I_{gt}\underline{C_g}+\sum_{j\in\mathcal{J}}m_{jg}P_{jgt}+C_{gt}^{SU}+C_{gt}^{SD}+\mu_g^R R_{gt}\right)\right.$$
$$\left.+\sum_{e\in\mathcal{E}}\left(C_e P_{et}^D+\mu_e^R R_{et}\right)\right]\quad (5)$$

where I_{gt} is a binary variable represents the commitment status of conventional generating unit g at time t; C_g is the minimum generation cost of unit g, and C_{gt}^{SU}, and C_{gt}^{SD} are the start up and shot down costs of unit g at time t, respectively; e_{jg} and P_{jgt} are the slope and corresponding power generation in block j of the considered piecewise linear generation cost function of unit g at time t; C_e and P_{et}^D are the variable cost and discharged power from energy storage e at time t; and R_{gt} and R_{et} are the reserve capacities scheduled for generating unit g and energy storage e at time t, respectively, with the corresponding reserve prices of μ_g^R and μ_e^R.

The objective function (5) is subject to prevailing thermal generating units, RESs injections and charging/discharging, and dynamic energy balance of ESSs, transmission grid, and system constraints:

$$P_{gt}=I_{gt}\underline{P_g}+\sum_{j\in\mathcal{J}}P_{jgt}\quad\forall g,t\quad (6)$$

$$0\le P_{jgt}\le\overline{P_{jg}}\quad\forall j,g,t\quad (7)$$

$$I_{gt}\underline{P_g}\le P_{gt}\le I_{gt}\overline{P_g}\quad\forall g,t\quad (8)$$

$$0\le R_{gt}\le I_{gt}\overline{R_g}\quad\forall g,t\quad (9)$$

$$0\le P_{wt}\le\overline{P_{wt}}\quad\forall w,t\quad (10)$$

$$0\le P_{st}\le\overline{P_{st}}\quad\forall s,t\quad (11)$$

$$C_{gt}^{SU} \geq SUC_g(I_{gt} - I_{g(t-1)}) \quad \forall g, t \tag{12}$$

$$C_{gt}^{SD} \geq SDC_g(I_{g(t-1)} - I_{gt}) \quad \forall g, t \tag{13}$$

$$P_{gt} - P_{g(t-1)} \leq P_g^{RU} I_{g(t-1)} + SUR_g(I_{gt} - I_{g(t-1)})$$
$$+ \overline{P_g}(1 - I_{gt}) \quad \forall g, t \tag{14}$$

$$P_{g(t-1)} - P_{gt} \leq P_g^{RD} I_{gt} + SDR_g(I_{g(t-1)} - I_{gt})$$
$$+ \overline{P_g}(1 - I_{g(t-1)}) \quad \forall g, t \tag{15}$$

$$\sum_{\substack{t'=t \\ t=1...|\mathcal{T}|-T_g^{on}+1}}^{t+T_g^{on}-1} I_{gt'} \geq T_g^{on}(I_{gt} - I_{g(t-1)}) \quad \forall g \tag{16}$$

$$\sum_{\substack{t'=t \\ t=1...|\mathcal{T}|-T_g^{off}+1}}^{t+T_g^{off}-1} (1 - I_{gt'}) \geq T_g^{off}(I_{g(t-1)} - I_{gt}) \forall g \tag{17}$$

$$0 \leq P_{et}^C \leq \beta_{et}\overline{P_e} \quad \forall e, t \tag{18}$$

$$0 \leq P_{et}^D + R_{et} \leq (1 - \beta_{et})\overline{P_e} \quad \forall e, t \tag{19}$$

$$0 \leq R_{et} \leq (1 - \beta_{et})\overline{R_e} \quad \forall e, t \tag{20}$$

$$E_{et} = E_{e(t-1)} + \left(\eta_e^C P_{et}^C - \frac{P_{et}^D}{\eta_e^D}\right)\Delta t \quad \forall e, t \tag{21}$$

$$\underline{E_e} \leq E_{et} \leq \overline{E_e} \quad \forall e, t \tag{22}$$

$$\sum_{g\in\mathcal{G}(b)} P_{gt} + \sum_{w\in\mathcal{W}(b)} P_{wt} + \sum_{s\in\mathcal{S}(b)} P_{st}$$
$$+ \sum_{e\in\mathcal{E}(b)} (P_{et}^D - P_{et}^C) - D_{bt} = \sum_{l\in\mathcal{L}(b)} P_{lt} \quad \forall b, t \tag{23}$$

$$-\overline{P_l} \leq P_{lt} \leq \overline{P_l} \quad \forall l, t \tag{24}$$

$$P_{lt} - B_l\left(\theta_{lt}^S - \theta_{lt}^R\right) = 0 \quad \forall l, t \tag{25}$$

$$\sum_{g\in\mathcal{G}} R_{gt} + \sum_{e\in\mathcal{E}} R_{et} \geq R_t \quad \forall t \tag{26}$$

$$I_{gt}, \beta_{et} \in \{0, 1\} \quad \forall g, e, t \tag{27}$$

Constraints (6)-(9) and (12)-(17) model the thermal generating units operation including min/max generation and reserve capacities, start-up and shot down costs, ramp up and down and on/off limits. Constraints (10) and (11) restrict captured wind and solar power generations to their maximum available amounts. Constraints (18)-(22) model ESSs charging/discharging events and dynamic energy balance that is bounded by min/max rated power, energy and dedicated reserve capacities. The power balance equation, transmission network, and system reserve requirement constraints are reflected in (23)-(27).

REFERENCES

[1] V. Stevenson, "Use of storage and renewable electricity generation to reduce domestic and transport carbon emissions-whole life energy, carbon and cost analysis of single dwelling case study (U.K.)," in *Proc. MDPI*, 2022, pp. 95–130.

[2] P. Denholm, P. Brown, W. Cole, T. Mai, B. Sergi, M. Brown, P. Jadun, J. Ho, J. Mayernik, C. McMillan, and others, "Examining supply-side options to achieve 100% clean electricity by 2035," Nat. Renew. Energy Lab. (NREL), Golden, CO, USA, Tech. Rep. NREL/TP-6A40-81644, 2022.

[3] N. Kittner, F. Lill, and D. M. Kammen, "Energy storage deployment and innovation for the clean energy transition," *Nature Energy*, vol. 2, no. 9, pp. 1–6, Jul. 2017.

[4] J. Aleluia, P. Tharakan, A. P. Chikkatur, G. Shrimali, and X. Chen, "Accelerating a clean energy transition in Southeast Asia: Role of governments and public policy," *Renew. Sustain. Energy Rev.*, vol. 159, May 2022, Art. no. 112226.

[5] I. Khan, A. Zakari, J. Zhang, V. Dagar, and S. Singh, "A study of trilemma energy balance, clean energy transitions, and economic expansion in the midst of environmental sustainability: New insights from three trilemma leadership," *Energy*, vol. 248, Jun. 2022, Art. no. 123619.

[6] O. Castrejon-Campos, L. Aye, and F. K. P. Hui, "Making policy mixes more robust: An integrative and interdisciplinary approach for clean energy transitions," *Energy Res. Social Sci.*, vol. 64, Jun. 2020, Art. no. 101425.

[7] F. Angizeh, A. Ghofrani, and M. A. Jafari, "Higher granular sectoral demand forecast under data scarcity: An integrated physics-based top–down and bottom–up approach," *IEEE Syst. J.*, vol. 16, no. 2, pp. 2923–2933, Jun. 2022.

[8] *PVWatts Calculator*, Nat. Renew. Energy Lab. (NREL), Golden, CO, USA, 2022. [Online]. Available: http://pvwatts.nrel.gov/pvwatts.php

[9] *Atlantic Shores Buoys, Atlantic Shores OffshoreWind*, Atlantic Shores Offshore Wind LLC, Brooklyn, NY, USA, 2022. [Online]. Available: https://www.atlanticshoreswind.com

[10] C. Williams and C. Rasmussen, "Gaussian processes for regression," in *Proc. Adv. Neural Inf. Process. Syst.*, vol. 8, 1995, pp. 1–7.

[11] New Jersey Energy Master Plan: Pathway to 2050. (2019). *The New Jersey Board of Public Utilities (NJBPU)*. [Online]. Available: https://nj.gov/emp/docs/pdf/2020_NJBPU_EMP.pdf

[12] New York Senate. (2019). *Senate Bill S6599–Climate Leadership & Community Protection Act*. [Online]. Available: https://www.nysenate.gov/legislation/bills/2019/s6599

[13] *IBM Software Group*, CPLEX, IBM ILOG, User-Manual CPLEX, vol. 12, 2018. [Online]. Available: http://www.ilog.com/products/cplex

[14] (2022). *Generation Capacity by Fuel Type, System Operations, PJM Interconnection*. [Online]. Available: https://www.pjm.com/markets-and-operations/ops-analysis.aspx

[15] *U.S. Energy Information Administration (EIA)*, Electric Power Annual 2021, U.S. Dept. Energy, Washington, DC, USA, 2022. [Online]. Available: https://www.eia.gov/electricity/annual/pdf/epa.pdf

[16] *New Jersey Energy Storage Analysis (ESA): Responses to the ESA Elements of the Clean Energy Act of 2018*, Rutgers, The State University of New Jersey, State New Jersey Board Public Utilities (NJBPU), Trenton, NJ, USA, 2019.

[17] *Load & Capacity Data (Gold Book)*, New York Independent System Operator (NYISO), New York, NY, USA, 2022.

[18] *New York's 6 GW Energy Storage Roadmap: Policy Options for Continued Growth in Energy Storage*, New York State Energy Research and Development Authority (NYSERDA), Albany, NY, USA, 2022.

FARHAD ANGIZEH (Member, IEEE) received the B.Sc. degree in electrical engineering from the Amirkabir University of Technology (Tehran Polytechnic), Tehran, Iran, in 2011, and the M.Sc. degree in energy systems engineering from the Sharif University of Technology, Tehran, Iran, in 2014, and the Ph.D. degree in industrial and systems engineering from Rutgers University, New Brunswick, NJ, USA, in 2023. He is currently a Post-Doctoral Associate with the Institute for Data, Systems, and Society at Massachusetts Institute of Technology, Cambridge, MA, USA. His research interests include demand response and energy management, modeling and integration of distributed and renewable energy resources, and optimization of smart electricity grids. He was a recipient of the IEEE Power and Energy Society (PES) Innovative Smart Grid Technologies (ISGT) North America Conference Best Paper Award, in 2021.

JINWOO BAE (Student Member, IEEE) received the B.Sc. degree in industrial and management systems engineering from Kyung Hee University, Republic of Korea, in 2016, and the M.Sc. degree in industrial and manufacturing engineering from the University of Wisconsin-Milwaukee, WI, USA, in 2019. He is currently pursuing the Ph.D. degree in industrial and systems engineering with Rutgers University, NJ, USA. His research interests include reliability and uncertainty of estimation from machine learning models, especially in computer vision, robot navigation, and prognostics.
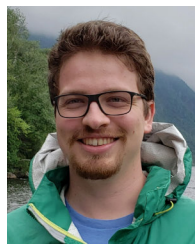
ALEXANDER KLEBNIKOV received the B.Sc. and M.Sc. degrees in mechanical engineering from the University of Pennsylvania, in 2016. He worked multiple roles as an Operations, Maintenance and Pressure Equipment Engineer with the Shell Deer Park Refinery, Houston, TX, USA, and Shell Ursa TLP, Gulf of Mexico. He is currently the Project Manager of Atlantic Shores Offshore Wind. His research interests include amorphous plasticity mechanics, wave energy and desalination, hydrogen, and energy policy.

JOYCE CHEN received the master's degree in international business from Queen's University, Canada. She has worked across the USA, Canada, The Netherlands, and China, including leading Corporate M&A activities of major renewable company acquisitions, energy market for new country entry, and major divestment program and a Venture Investor in renewable power, hydrogen, storage, and mobility for shell. Currently, she is the Commercial and Finance manager for Atlantic Shores Offshore Wind.

MOHSEN A. JAFARI (Member, IEEE) received the Ph.D. degree from Syracuse University, in 1985. He has directed or co-directed a total of over 23 million U.S. dollars in funding from various government agencies, including the National Science Foundation, the Department of Energy, the Office of Naval Research, the Defense Logistics Agency, the NJ Department of Transportation, FHWA, and industry in automation, system optimization, data modeling, information systems, and cyber risk analysis. He actively collaborates with universities and research institutes abroad. He has also been a Consultant to several Fortune 500 companies and local and state government agencies. He is currently a Professor and the Chair of Industrial and Systems Engineering with Rutgers University–New Brunswick. His research interests include manufacturing, transportation, healthcare, and energy systems. He is a member of IIE. He received the IEEE Excellence Award in service and research.

• • •